Continuous Monitoring of Rice Growth With a Stable Ground-Based Scatterometer System

Yihyun Kim, Hoonyol Lee, and Sukyoung Hong

***Abstract*—Ground-based polarimetric scatterometers have been effective tools to monitor the growth of rice crop, with much higher temporal resolution than satellite synthetic aperture radar systems. However, scatterometer data obtained in every few days, as were the case for the previously reported studies, were not enough to address the effects of ever-changing weather conditions. In this letter, we constructed a highly stable X-, C-, and L-bands polarimetric scatterometer system in an air-conditioned shelter. The incidence and azimuth angles of the antenna were fixed to 40° and 0°, respectively, to avoid uncertainty in repositioning error. Season-long daily backscattering coefficients from transplanting to harvesting were compared with rice growth data. Total fresh weight, leaf area index, and plant height were highly correlated with L-HH (0.97, 0.96, and 0.88, respectively) due to the deeper penetration and the dominance of double bounce in lower frequency. High-quality backscattering data clearly revealed the dual-peaked pattern in X-band, among which X-VV correlated best with grain dry weight and gravimetric grain water content (0.94 and 0.92, respectively) due to the better interaction of grain and rice canopy with microwave of higher frequency. These results will be useful in retrieving crop biophysical properties and determining the optimum microwave frequency and polarization necessary to monitor crop conditions.**

***Index Terms*—Backscattering coefficients, grain dry weight (GDW), gravimetric grain water content (GWCg), leaf area index (LAI), plant height, polarimetric scatterometer, rice, total fresh weight (TFW).**

I. Introduction

RICE is a primary food source for more than half of the world's population. Satellite synthetic aperture radar (SAR) has been widely used to monitor biophysical conditions of various crops over a large area [1]–[6]. Particularly for rice, various rice growth parameters were found to be closely correlated with backscattering coefficients in various radar frequencies and polarizations. Retrieving radar backscattering from paddy rice field is vulnerable to weather conditions primarily due to the motion of crops and moisture contents, as well as wind-blown undulating water surface. Therefore, the requirement of temporal resolution in data acquisition for a flooded rice paddy field can be significantly higher than those of the existing satellite SAR systems.

Manuscript received May 11, 2012; revised August 23, 2012; accepted October 15, 2012.

Y. Kim is with the National Academy of Agricultural Science, Rural Development Administration, Suwon 441-707, Korea, and also with the Department of Geophysics, Kangwon National University, Chuncheon 200-701, Korea.

H. Lee is with the Department of Geophysics, Kangwon National University, Chuncheon 200-701, Korea.

S. Hong is with the National Academy of Agricultural Science, Rural Development Administration, Suwon 441-707, Korea.

Digital Object Identifier 10.1109/LGRS.2012.2225595

Several researchers have attempted to construct ground-based polarimetric scatterometers to increase the temporal resolution of rice backscattering data [7]–[9]. However, previous studies were not enough to fully investigate the effects of weather on radar backscattering. Ever-changing wind moves plant leaves and stems during a sweep time of a vector network analyzer (VNA) operating in stepped-frequency mode. Radar backscattering can significantly degrade if a target or a system is not stable enough during the sweep time, which is on the order of 0.1 to several seconds, depending on the settings of the VNA.

In this letter, we report a season-long measurement of radar backscattering of a rice paddy field using an X-, C-, and L-bands polarimetric scatterometer with much higher accuracy than previous studies [7]–[9]. Section II describes the study site, methods to obtain various rice growth data, and a highly stable polarimetric scatterometer system. The system automatically and continuously operated in every 10 min to assess the frequency and polarization dependency of radar backscattering over the entire rice growth period. All system components were put in an air-conditioned shelter to minimize the effects of temperature, rain, humidity, and wind to the radio frequency (RF) system. We analyzed the interaction between X-, C-, and L-bands signatures and biophysical measurements in Section III. Conclusions with summaries of the findings are given in Section IV.

II. Method

A. Study Site and Rice Growth Data

The study site is located at an experimental field of the National Academy of Agricultural Science, Suwon, Korea (Latitude $37°15'28.0''$ N, Longitude $126°59'21.5''$ E). The paddy field was flooded and transplanted with rice seedlings (*Oryza sativa* L. *japonica*, Variety: Chuchung byeo) on May 18, 2009. A set of three seedlings of approximately 15-cm long was planted at 15-cm spacing in a row, with 30-cm row spacing. The paddy field has been flooded until September 14, 2009 and then drained afterward. Rice was harvested on October 12, 2009, 147 days after transplanting (DAT).

Rice growth data were acquired once a week by collecting three clusters of rice plants in a destructive way. Rice plants were dissembled into leaves, stems, and grains and separately weighed. Total fresh weight (TFW) and grain fresh weight (GFW) were calculated in $g \cdot m^{-2}$ as a ratio of fresh biomass and fresh grain, respectively, to rice cluster area. Leaf area index (LAI) was measured as a dimensionless ratio of total leaf area, which is measured by LI-3100 (LI-COR, Inc.), to rice cluster

TABLE I
SPECIFICATION OF THE X-, C-, AND L-BAND AUTOMATIC SCATTEROMETER SYSTEM

Parameters		X-Band	C-Band	L-Band
Frequency (GHz)		9.65±0.5	5.3±0.3	1.27±0.06
Beam width	E-Plane (Deg.)	11	12	41
	H-Plane (Deg.)	16	17	60
Number of Frequency Points		1601	801	201
Antenna Type		Dual polarimetric square horn		
Antenna Gain (dB)		22.4	20.1	12.4
Slant Range Resolution (m)		0.15	0.25	1.25
Band Width (MHz)		1000	600	120
Wavelength (m)		0.031	0.056	0.23
Polarization		HH, HV, VH, VV		
Incident Angle (°)		40		
Platform Height (m)		4.16		
Measurement interval		10 minutes		
Sweep Time (s)		1.8	0.9	0.225

area. Rice plants were then dried in an oven for 36 h at 60 °C to measure total dry weight and grain dry weight (GDW), all in $g \cdot m^{-2}$. Gravimetric water content and volumetric grain water content (GWCg and GWCv, respectively) were calculated as follows:

$$\mathrm{GWCg} = \mathrm{GFW} - \mathrm{GDW}\ (\mathrm{g} \cdot \mathrm{m}^{-2}) \quad (1)$$

$$\mathrm{GWCv} = (\mathrm{GFW} - \mathrm{GDW})/\mathrm{GFW} \times 100(\%). \quad (2)$$

B. Polarimetric Scatterometer System

The polarimetric scatterometer consists of a vector network analyzer (Agilent 8720D), a microwave switch, RF cables, a power unit, and a personal computer (see Table I). All components were installed inside an air-conditioned shelter to maintain constant temperature and humidity during the whole acquisition period. Three antennas for X-, C-, and L-bands, respectively, were extruded outside of the shelter at a fixed incidence angle of 40° and at a height of 4.16 m from the ground. The choice of a fixed incidence angle (and a fixed azimuth angle of zero) was for the sake of system stability based on the result of our previous study [8]. The direction of radar line of sight was perpendicular to the orientation of the rows of rice plants. Field of view measures 2.0 m in ground range and 1.1 m in azimuth direction for X-band, 2.2 m × 1.2 m for C-band, and 7.4 m × 3.9 m for L-band.

Center frequencies of the three antennas were designed to coincide with current satellite SAR systems for a possible comparison study in the future. Data from the VNA-based polarimetric scatterometer were obtained in a stepped-frequency sweep mode. The system and the target should be structurally stable during the sweep time, or the stepped-frequency mode fails to constitute radar and thus degrades the backscattering signal. The data were transformed into time domain via inverse Fourier transformation and then appropriately time gated to obtain S-parameter. Backscattering coefficients (σ°) were then calculated by applying the radar equation in [10].

The system was designed to automatically measure fully polarimetric backscattering coefficients of rice field in X-, C-, and L-bands in every 10 min. Daily standard deviations of backscattering coefficients were measured to be 2–4 dB, depending on weather effect. Therefore, a daily maximum was selected out of 144 measurements per day to represent the daily backscattering coefficient of rice paddy field. This is based on an assumption that wind degrades the backscattering of radar operating in stepped-frequency mode so that the daily maximum occurs when the wind speed is minimal. The daily standard deviation of previous studies in [8] and [9], where there was no statistically meaningful number of measurement in a day, was estimated to be 2–4 dB as well by calculating the standard deviation between the data and a linear regression function within a moving window of a few days. In that sense, we can say that the accuracy of our daily maximum data, as calculated by the same moving window method, is less than 1 dB, whereas those in [8] and [9] and our "raw" data are 2–4 dB.

Pauli decomposition was applied to separate backscattering mechanisms into single (odd) bounce, double (even) bounce, and volume scattering [11]. In case of matured rice plants, single bound dominates when radar is reflected from canopy top. Double bounce occurs when radar signal is reflected once on water surface and bounced again on stems and leaves. Volume scattering happens when the penetration of microwave through plant canopy is allowed. Such scattering mechanisms are all dependent on the frequency and polarization of the incident microwave.

III. ANALYSIS

A. Seasonal Variations of Rice Growth Data and Radar Backscattering

Highly stable daily backscattering data obtained in this experiment enable more detailed analysis of rice growth stages when compared with various rice growth data. Fig. 1 depicts

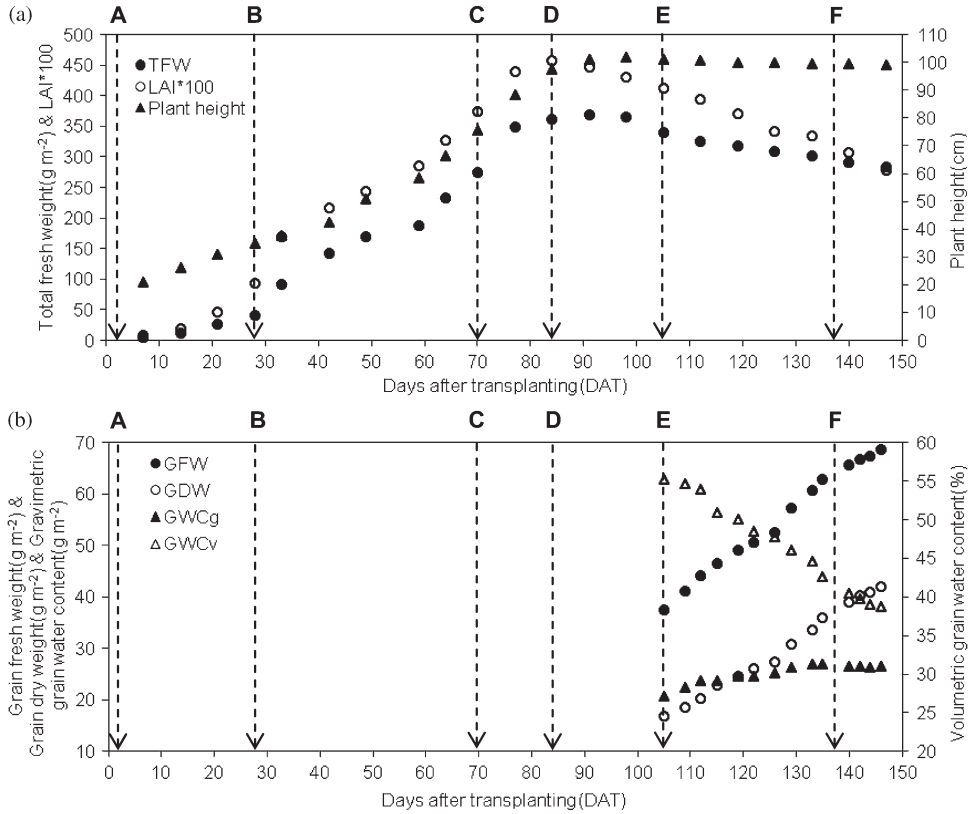

Fig. 1. Rice growth data during the whole rice growth period. (a) TFW, LAI, and plant height. (b) GFW, GDW, GWCg, and GWCv.

season-long rice growth data and radar backscattering data. Rice growth period can be divided into three major growth stages [12] as follows: 1) *vegetative stage* from transplant (A, DAT 3) through effective tillering (B, DAT 28) and to panicle formation (C, DAT 70); 2) *reproductive stage* from panicle formation to heading (D, DAT 84); and 3) *ripening stage* from heading through soft dough (soft grain) stage (E, DAT 105), overripe (hard grain) stage (F, DAT 137), and to full maturity (DAT 147). The DAT of every stage was defined as a date when the corresponding phenomenon dominantly appears by approximately 50% of the whole rice population.

Fig. 1(a) shows that plant height reached at its maximum of 1 m at heading and remained constant afterward. TFW and LAI gradually increased until heading (D, DAT 84) and declined thereafter. GFW and GDW increased, but GWCv monotonically decreased from heading to harvesting, as shown in Fig. 1(b). However, GWCg reached its maximum at overripe stage (F, DAT 137) and then gradually decreased.

Fig. 2 shows that backscattering gradually increased in all bands and polarizations, in accordance with the rice growth data, and then decreased mainly due to the reduction in LAI and TFW. However, the dates of maximum backscattering were frequency dependent, i.e., DAT 68 for X-band (close to panicle formation) and DAT 82 (close to heading stage) for both C- and L-bands. The phenomenon of delayed peak for C- and L-bands is related to the higher penetration capability of lower frequency microwave into rice canopy.

Contrary to C- and L-bands that monotonously decreased after heading to harvesting, X-band showed a rather complex pattern. Backscattering increased again from the soft dough stage (E, DAT 105) to the overripe stage (F, DAT 137) and then decreased afterward until full maturity. This dual peakness of X-band data was clearly detected in this experiment, which was not obvious in the previous studies (see [8] and [9]).

The decrease from C to E follows the decrease in LAI and TFW, which is similar to C- and L-bands. The following increase in backscattering from E to F indicates that the formation and growth of grains were captured only by higher frequency (X-band, in this case) probably because the size and structure of rice heads are comparable with shorter wavelength. However, the decrease in backscattering from the overripe stage (F, DAT 137) to harvesting tells another story. X-band backscattering followed the peaked pattern of GWCg rather than the monotonic changes of GFW, GDW, or GWCv. GWCg increases from the soft dough stage (E, DAT 105) to the overripe stage (F, DAT 137) and decreased thereafter until full maturity. This implies that X-band backscattering is sensitive to the net amount of water captured inside the grain (GWCg) as well as the dry matter of the grain. This is an important finding from our experiment in that we have identified a similar pattern between X-band and GWCg for the first time.

Fig. 3 is the Pauli decomposition of the backscattering data showing single bounce (α), double bounce (β), and volume scattering (γ). Among them, single bounce is dominant for all stages and in all bands. Double bounce and volume scattering approximately equal in C-band. For L-band, double bounce from flooded water and stems dominates over volume scattering from leaves $(\beta > \gamma)$ due to the deeper penetration of longer wavelength into rice canopy. On the other hand, volume scattering is more significant than double bounce for X-band $(\beta < \gamma)$.

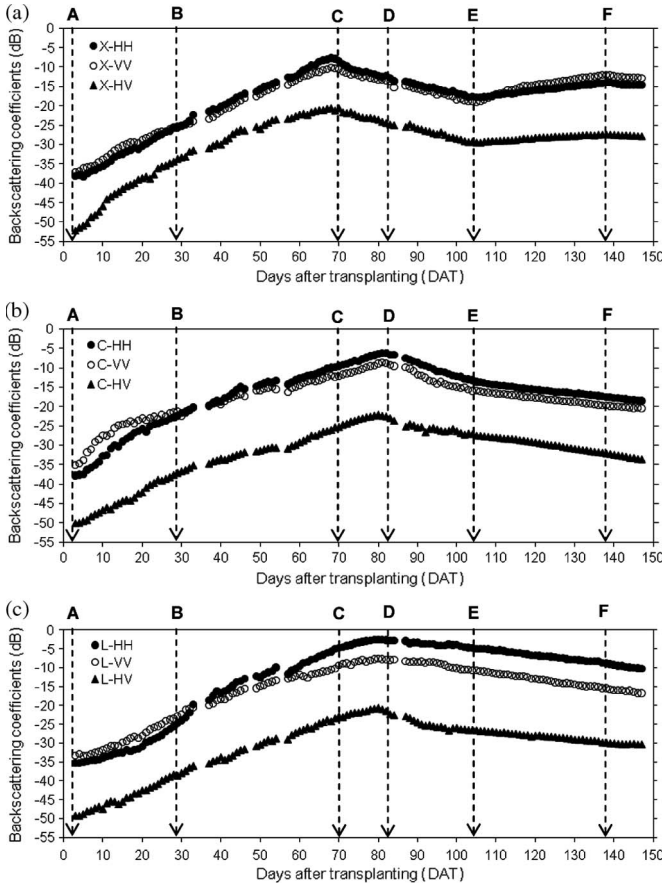

Fig. 2. Daily backscattering coefficients of HH, VV, and HV channels during the whole rice growth period in (a) X-, (b) C-, and (c) L-bands.

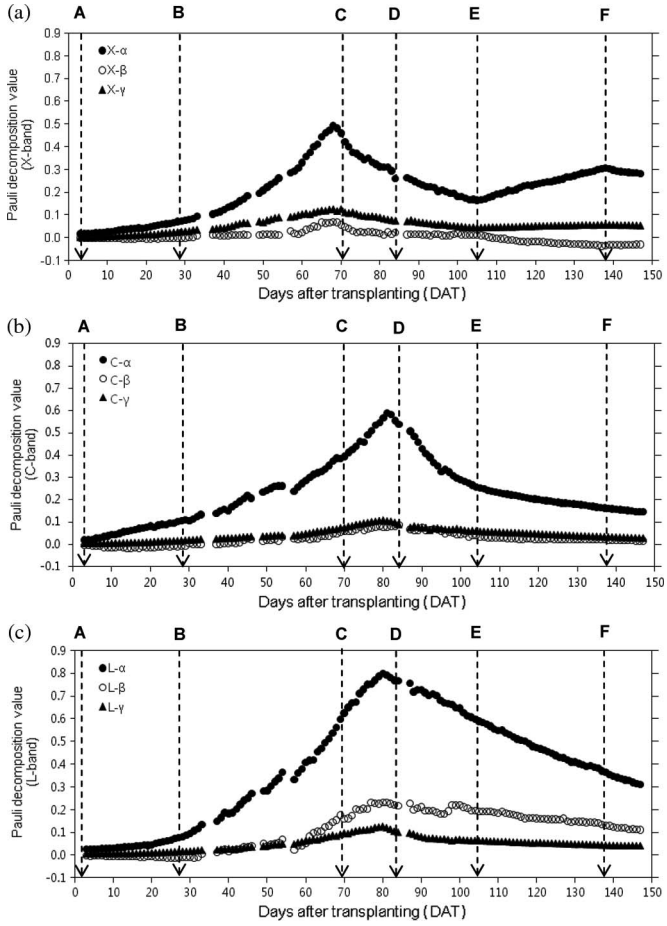

Fig. 3. Components of Pauli decomposition (α, β, and γ) in (a) X-, (b) C-, and (c) L-bands.

B. Correlations Between Rice Growth Data and Radar Backscattering

Table II shows the results of correlation analysis between rice growth data and the backscattering coefficients of X-, C-, and L-bands in various polarizations. The highest correlation coefficient for TFW was found with L-HH (0.97), whereas other channels showed relatively good positive correlation (0.73–0.89). LAI was highly correlated with L-HH (0.96) and was in good positive correlation with other polarizations of L- and C-bands (0.84–0.91). However, the dual-peaked X-band was less correlated with LAI, which monotonically decreased after heading (0.66–0.72), which implies that higher frequency strongly interacts with GWC during the ripening stage. Plant height was best correlated with L-HH (0.88) and other polarizations of L-band (0.78–0.80) but less correlated with C-band (0.60–0.77) and X-band (0.63–0.79). Plant height remained almost constant after heading, which resembles the pattern of L-band rather than C- or X-bands.

Generally, higher frequency (X-VV in this case) was weakly correlated with TFW, LAI, and plant height but correlated well with GDW (0.94) and GWCg (0.92). The good correlation between X-band and GWCg was newly found from this experiment due to the higher temporal resolution of the scatterometer data. C- and L-bands showed weak correlation with grain parameters, indicating that lower frequency does not interact much with grains.

IV. Conclusion

Near-continuous acquisition of backscattering coefficients in every 10 min by using an X-, C-, and L-bands polarimetric scatterometer system enabled us to accurately assess the frequency and polarization dependency of radar backscattering in various rice growing stages.

Comparison of the seasonal variations between daily backscattering data and rice growth data confirmed the following properties of microwave interactions with rice with much higher accuracy than previous studies (see [8] and [9]): 1) The penetration of microwave into rice canopy stems was deeper in lower frequency (L- and C-bands), whereas the interactions with grains were better in higher frequency (X-band); 2) the peak date of the backscattering of X-band precedes those of C- or L-bands by 14 days; 3) double bounce (β in Pauli decomposition) is stronger than volume scattering (γ) for L-band, whereas the opposite is the case for X-band; and 4) X-band is sensitive to GWCg so that it showed the dual peakness (the first peak on 68 DAT and the second peak on 137 DAT) of the backscattering during the rice growing season.

Correlation analysis between backscattering and rice growth data revealed that lower frequency bands (C- and L-bands) are closely related with the mass information of the whole canopy such as TFW, LAI, and plant height; whereas higher frequency band (X-band) correlated well with grain weight

TABLE II
CORRELATION COEFFICIENTS BETWEEN THE BACKSCATTERING OF X-, C-, AND L-BANDS IN FULL-POLARIZATION AND VARIOUS RICE GROWTH PARAMETERS. THE MAXIMUM CORRELATIONS ARE HIGHLIGHTED IN BOLD CHARACTER FOR EACH RICE GROWTH PARAMETER AND RADAR CHANNELS

Growth Data	X-band (dB)			C-band (dB)			L-band (dB)		
	HH	VV	HV	HH	VV	HV	HH	VV	HV
TFW (g m^{-2})	0.81	0.73	0.83	0.84	0.75	0.88	**0.97**	0.87	0.89
LAI	0.72	0.66	0.68	0.90	0.86	0.91	**0.96**	0.84	0.91
Plant Height (cm)	0.72	0.63	0.79	0.73	0.60	0.77	**0.88**	0.80	0.79
GDW	0.81	**0.94**	0.70	-0.62	-0.60	-0.64	-0.57	-0.53	-0.62
GWCg (g m^{-2})	0.83	**0.92**	0.76	-0.56	-0.58	-0.50	-0.58	-0.55	-0.54
GWCv (%)	-0.85	**-0.89**	-0.82	0.60	0.59	0.58	0.62	0.61	0.60

and grain water content. Particularly from this experiment, at a fixed incidence angle of 40°, it was suggested that L-HH is the most preferable channel for the monitoring of TFW (0.97), LAI (0.96), and plant height (0.88); whereas X-VV was best for GDW (0.94) and GWCg (0.92). Those results can be useful in determining RF frequency and polarization of future satellite SAR systems and in designing a ground-based microwave system for long-term monitoring of rice paddy field.

ACKNOWLEDGMENT

This work was carried out with the support of "Cooperative Research Program for Agriculture Science & Technology Development (Project PJ007753032012)" by Rural Development Administration, Korea.

REFERENCES

[1] T. Le Toan, H. Laur, E. Mougin, and A. Lopes, "Multitemporal and dual-polarization observations of agricultural vegetation covers by X-band SAR images," *IEEE Trans. Geosci. Remote Sens.*, vol. 27, no. 6, pp. 709–718, Nov. 1989.

[2] T. Kurosu, M. Fujita, and K. Chiba, "The identification of rice fields using multi-temporal ERS-1 C-band SAR data," *Int. J. Remote Sens.*, vol. 18, no. 14, pp. 2953–2965, Sep. 1997.

[3] J. P. Wigeron, P. Ferrazzoli, A. Olioso, P. Bertuzzi, and A. Chanzy, "A simple approach to monitor crop biomass from C-band radar data," *Remote Sens. Environ.*, vol. 69, no. 2, pp. 179–188, Aug. 1999.

[4] G. Macelloni, S. Paloscia, P. Pamaloni, F. Marliani, and M. Gai, "The relationship between the backscattering coefficient and the biomass of narrow and broad leaf crops," *IEEE Trans. Geosci. Remote Sens.*, vol. 39, no. 4, pp. 873–884, Apr. 2001.

[5] J. Chen, H. Lin, and Z. Pei, "Application of ENVISAT ASAR data in mapping rice crop growth in Southern China," *IEEE Geosci. Remote Sens. Lett.*, vol. 4, no. 3, pp. 431–435, Jul. 2007.

[6] A. Bouvet, T. Le Toan, and N. Lam-Dao, "Monitoring of the rice cropping system in the Mekong Delta using ENVISAT/ASAR dual polarization data," *IEEE Trans. Geosci. Remote Sens.*, vol. 47, no. 2, pp. 517–526, Feb. 2009.

[7] S. B. Kim, B. W. Kim, Y. K. Kang, and Y. S. Kim, "Radar backscattering measurements of rice crop using X-band scatterometer," *IEEE Trans. Geosci. Remote Sens.*, vol. 38, no. 3, pp. 1467–1471, May 2000.

[8] Y. H. Kim, S. Y. Hong, and H. Y. Lee, "Estimation of paddy rice growth parameters using L, C, X-bands polarimetric scatterometer," *Korean J. Remote Sens.*, vol. 25, no. 1, pp. 31–44, 2009.

[9] Y. Inoue, T. Kurosy, H. Maeno, S. Uratsuka, T. Kozu, K. Dabrowka-Zielinska, and J. Qi, "Season-long daily measurements of multifrequency (Ka, Ku, X, C, and L) and full-polarization backscatter signatures over paddy rice field and their relationship with biological variables," *Remote Sens. Environ.*, vol. 81, no. 2/3, pp. 194–204, Aug. 2002.

[10] F. T. Ulaby and C. Elachi, *Radar Polarimetry for Geoscience Applications*. Norwood, MA: Artech House, 1990.

[11] S. R. Cloude and E. Pottier, "A review of target decomposition theorems in radar polarimetry," *IEEE Trans. Geosci. Remote Sens.*, vol. 34, no. 2, pp. 498–518, Mar. 1996.

[12] U. Meier, *Growth Stages of Mono- and Dicotyledonous Plants: BBCH Monograph*, 2nd ed. Berlin, Germany: Blackwell Wissenschafts, 2001.